Future Medicinal Chemistry

Ephedrine as a lead compound for the development of new DPP-IV inhibitors

Journal:	*Future Medicinal Chemistry*
Manuscript ID	FMC-2017-0080.R1
Manuscript Type:	Short Communication
Keywords:	Ephedra extract, natural compounds, protein-ligand docking

Ephedrine as a lead compound for the development of new DPP-IV inhibitors

Abstract

Background: Extracts from *Ephedra* species have been reported to be effective as antidiabetics. A previous *in silico* study predicted that ephedrine and five ephedrine derivatives could contribute to the described antidiabetic effect of *Ephedra* extracts by inhibiting dipeptidyl peptidase IV (DPP-IV). Finding selective DPP-IV inhibitors is a current therapeutic strategy for type 2 diabetes mellitus management. Therefore, the main aim of this work is to experimentally determine whether these alkaloids are DPP-IV inhibitors.

Results: Our results show that all six molecules are DPP-IV inhibitors, with IC_{50} ranging from 124 μM for ephedrine to 28.890 mM for N-methylpseudoephedrine.

Conclusions: Further computational analysis shows how *Ephedra*'s alkaloids could be used as promising lead molecules for designing more potent and selective DPP-IV inhibitors.

Keywords: Ephedra extract; natural compounds; protein-ligand docking

1. Introduction

Nature has been an essential resource in folk medicine for the treatment of a wide variety of diseases. Moreover, in recent decades, medicinal chemists have used the complexity and molecular diversity of natural products to discover and develop new drugs [1,2]▪. Of all small-molecule approved drugs between 1981 and 2014, 33% are either natural products or have been derived from them [3]▪. Plants in particular have played an important role in healthcare for different cultures. For instance, about 800 medicinal plants have been reported to show hypoglycemic properties [2,4]▪.

Plants from the *Ephedra* family, whose traditional preparation is called *ma huang*, have been used in Chinese medicine for over 5000 years as a circulatory stimulant, a diaphoretic and an antipyretic remedy [5]▪. Indeed, *Ephedra* was considered a spiritual drink for rejuvenation, immortality and resurrection in ancient Aryan culture [6]▪. *Ephedra* species contain alkaloids of biological relevance such as ephedrine, pseudoephedrine, norephedrine, norpseudoephedrine, N-methylephedrine and N-methylpseudoephedrine [7,8]▪; all which have a similar molecular structure. These alkaloids are adrenergic agonists that stimulate the release of endogenous catecholamines (see Table S1) [9–11]▪. For this reason, the *Ephedra* herb has been commonly used for increasing blood pressure and stimulating the central nervous system [9,10]▪. Likewise, it has benefits for the treatment of asthma, coughs, colds and mild forms of bronchospasm [11–13]▪. Unfortunately, consumption of this plant has been associated with various adverse effects including palpitations, hypertension, insomnia, anxiety and dysuria [10–13]▪. Because of these adverse cardiovascular effects and the fact that it is a major source of methamphetamine [5,8]▪, *Ephedra* extracts have been banned in food supplements in several European countries [14]▪ and by the American Food & Drug Administration (FDA) [5,10]▪.

Extracts from some *Ephedra* species (*i.e.*, *Ephedra sinica* and *Ephedra alata*) have been also reported to be effective as oral antidiabetics [15,16]▪. Moreover, it has been shown that they regenerate atrophied pancreatic islets and restore insulin secretion [16]▪. Interestingly, a recent computational study has predicted that ephedrine and other derivatives also present in different *Ephedra* species can inhibit the dipeptidyl peptidase-IV enzyme (DPP-IV) [17]▪. DPP-IV is a ubiquitous aminopeptidase that selectively removes N-terminal dipeptides from peptides with proline or alanine in the second position [18,19]▪. DPP-IV is involved in glycemia, cardiovascular function and inflammation through the proteolytic inactivation of a wide variety of biological regulatory peptides, including incretin hormones [20]▪. Incretins, secreted as a response to nutrient ingestion, play a key role in the regulation of glucose homeostasis and pancreatic islet functions [21]▪. Therefore, a good mechanism for treating or preventing type 2 diabetes mellitus (T2DM) could consist of inhibiting DPP-IV and thus increasing the half-lives of incretin hormones [18,21]▪. Consequently, DPP-IV inhibitors are of considerable interest to the pharmaceutical industry [19,22,23]▪, and intensive research in this area has resulted in the recent launch of several gliptins onto the market for T2DM treatment (see Table S2). Interestingly, DPP-IV inhibitors can also inhibit the apoptosis of β-cells and thus help them to regenerate and differentiate, which would have the same positive effect on islet pancreatic regeneration [24,25]▪ that has also been

described for *Ephedra* extracts [16]▪ . The selectivity of the DPP-IV inhibitors is also important for establishing an optimal safety profile for this antihyperglycemic treatment. Thus, the inhibition of DPP8 and DPP9 by DPP-IV inhibitors has been associated with multi-organ toxicities in preclinical species (*e.g.* alopecia, thrombocytopenia, reticulocytopenia, enlarged spleen, multi-organ histopathological changes, mortality in rats and gastrointestinal toxicity in dogs) [26]▪ .

Therefore, the main goals of the present study are **(1)** to demonstrate that, at least partly, the described antidiabetic effect of different *Ephedra* species extracts is the result of the DPP-IV inhibitory bioactivity of ephedrine and the ephedrine-derivatives found in these extracts; and **(2)** to perform a computational study to suggest how one of these alkaloids could be used as lead compound for designing new DPP-IV inhibitors with better potency and selectivity and without the side effects associated to ephedrine and the ephedrine-derivatives.

2. Experimental

2. 1. Chemicals and biochemicals

The compounds (1R,2S)-(-)-ephedrine (product number 134910), (1S,2S)-(+)-pseudoephedrine (product number 287636), (1S,2R)-(+)-norephedrine (product number 317500), (1R,2R)-(-)-norpseudoephedrine (product number 670561), (1R,2S)-(-)-N-methylephedrine (product number 235210) and (1S,2S)-(+)-N-methylpseudoephedrine (product number 290041) (purity ≥ 98%) were purchased from Sigma Aldrich (St Louis, MO). The DPP-IV Drug Discovery Kit-AK499 was purchased from Enzo Life Sciences International, Inc. (Farmingdale, NY) whereas the fluorogenic DPP8 (catalog number 80208) and DPP9 (catalog number 80209) assay kits were bought from BPS Bioscience, Inc. (San Diego, CA). Vildagliptin (purity ≥ 98%) was purchased from Cayman Chemical Company (Ann Arbor, MI).

2.2. Pure compound preparation

The first stock solution for pseudoephedrine and norpseudoephedrine was made with 99.9% ethanol, N-methylephedrine and N-methylpseudoephedrine were prepared with 99.9% methanol and ephedrine and norephedrine were prepared with 1M HCl solution. The rest of the dilution banks were made with 50 mM Trizma hydrochloride at pH 7.4.

2.3. In vitro assay of inhibition of DPP-IV by ephedrine and ephedrine-derivatives

The DPP-IV drug discovery Kit-AK499 was used to measure the DPP-IV inhibitory activity of ephedrine and ephedrine-derivatives. The DPP-IV activity was monitored fluorimetrically by using the fluorogenic substrate (*i.e.*, H-Gly-Pro-AMC) provided by the kit. This fluorimetric assay is based on the cleavage of the 7-amino-4-methylcoumarin moiety (*i.e.*, AMC) from the C-terminus of the peptide substrate, which

intensifies its fluorescence. The procedure was performed in a 96-well microplate in 100 µL of reaction volume. After the addition of 10 µL of each compound tested to the human recombinant DPP-IV enzyme, the microplate was incubated for 10 minutes at room temperature to allow compound/enzyme interaction. Next, the reaction was started by the addition of 50 µL (diluted 50-fold from stock) of the fluorimetric substrate H-Gly-Pro-AMC. Finally, sample triplicates were read each minute for 40 minutes in a Biotek FLx800 Fluorescence Microplate Reader at Ex:380nm/Em:460nm. Four different conditions were used: **(1)** the blank (*i.e.*, no DPP-IV present); **(2)** the negative control (*i.e.*, no inhibitor present); **(3)** the positive control (*i.e.*, the P32/98 inhibitor diluted 10-fold from stock provided by the kit); and **(4)** the ephedrine and ephedrine-derivatives at different concentrations (see Figure S1). Data was plotted as time versus Relative Fluorescence Units, and only the slope where the reaction was linear was used to obtain the activity of the enzyme. The remaining enzyme activity for DPP-IV in the presence of each tested compound was calculated as a percentage of activity relative to negative control wells.

2.4. In vitro assay of inhibition of DPP8 and DPP9 by ephedrine and ephedrine-derivatives

Similar fluorogenic assays were performed to measure DPP8 and DPP9 activity under the effect of ephedrine and ephedrine-derivatives. The procedure was performed in a 96-well black microplate in 100 µL of reaction volume. Briefly, after the addition of 10 µL of each compound tested to the human recombinant DPP8 and DPP9 enzyme, the microplate was incubated for 10 minutes at room temperature to allow compound/enzyme interaction. Next, the reaction was started by the addition of 20 µL (diluted 20-fold from stock) of the fluorigenic substrate. Finally, sample triplicates were read in a Biotek FLx800 Fluorescence Microplate Reader at Ex:380nm/Em:460nm. Four different conditions were used: **(1)** the blank (*i.e.*, no DPP8/DPP9 present); **(2)** the negative control (*i.e.*, no inhibitor present); **(3)** the positive control [*i.e.*, vildagliptin (with IC_{50} = 900 and 680 nM for DPP8 and DPP9, respectively) at 2.5 nM]; and **(4)** the ephedrine and ephedrine-derivatives at concentrations equal to their IC_{50} for DPP-IV. The remaining enzyme activity for DPP8 or DPP9 in the presence of each tested compound was calculated as a percentage of activity relative to negative control wells.

2.5. Statistical analysis and IC_{50} calculation

Statistical calculations were carried out with XLSTAT v2016.7 for Windows. Results were expressed as the mean ± SD of three replicates. The DPP-IV IC_{50} was obtained through non-linear regression (curve fit) followed by sigmoidal dose-response curve (variable slope). One-Way ANOVA followed by Bonferroni's Multiple Comparison Test were applied to observe significant differences ($p < 0.05$).

2.6. Target structure setup for protein-ligand docking

The protein structure used during the protein-ligand docking studies has the Protein Data Bank (PDB) code 1X70. Default options with VHELIBS were used to evaluate the correctness of the fit between the 1X70 binding site coordinates and the electron density map [27]. According to the results of this

analysis, the binding site coordinates for this structure are reliable and, therefore, suitable for use as the target during protein-ligand docking.

In order to set up 1X70 for use as a target during the protein-ligand docking with Glide v6.9 (Schrödinger, LLC, New York, NY, 2015), it was prepared with the *Protein Preparation Wizard* panel (PPW; Protein Preparation Wizard 2015-4, Schrödinger, LLC, New York, NY, 2015) available at the Schrödinger 2015-4 release. During the PPW's pre-process step all options were set to default with the exception of *remove original hydrogens*, *fill in missing side chains* and *cap termini* options that were set to on. During the PPW's *review and modify* step, chain B was removed and states for the 1X70's ligand were generated with default parameters. Then the S2 state for the ligand was chosen because it has a lower state penalty (*i.e.*, 0.83 Kcal/mol) and a higher H-bound count (*i.e.*, 2) compared with those of the original ligand state (*i.e.*, 4.00 Kcal/mol and 1, respectively). Finally, during the PPW's *refine* step: **(a)** hydrogen bond assignment was performed with default options with the *automatically optimize* tool; **(b)** waters with less than 3 hydrogen bonds to non-waters were removed; and **(c)** the resulting structure was submitted to a restrained minimization with default options.

The resulting 1X70 structure was then used to obtain the grid used during the docking of ephedrine and ephedrine-derivatives. The receptor grid was obtained around the 1X70's ligand (*i.e.*, sitagliptin) by using the *Schrödinger's Grid Generation* panel with default options.

2.7. Ephedrine and ephedrine-derivatives setup for protein-ligand docking

In order to obtain their 3D structures, ephedrine and ephedrine-derivatives were downloaded from Reaxys Medicinal Chemistry (http://www.reaxys.com). Then, all six molecules were processed with LigPrep v3.6 (Schrödinger, LLC, New York, NY, 2015) as follow: **(a)** the force field OPLS 2005 was used; **(b)** all possible ionization and tautomerization states at pH 7.0 ± 2.0 were generated with Epik; **(c)** the desalt option was activated; **(d)** chiralities were respected from input geometry when generating stereoisomers; and **(e)** one low-energy ring conformation per ligand was generated.

2.8. Structure-based pharmacophore generation for DPP-IV Inhibition

The structure-based pharmacophore used in the present study (see Figure S2A) is a modified version of a previous one developed by our group (see Figure S2B) [28]. Thus, Figure S2 shows that: **(a)** both pharmacophores share two compulsory sites (*i.e.*, **P/D** and **H/R1**) showing interactions with the Glu205/Glu206 dyad (*i.e.*, **P/D**) and with the S1 pocket (*i.e.*, **H/R1**); **(b)** the optional sites **H/R2** and **H/R4** are related with sites **R2** and **P/R3** in the new pharmacophore, respectively; and **(c)** the rest of the sites in the old pharmacophore are not shared either because of its preference to form covalent bonds (*i.e.*, **H/R3**) or because of their low energy contribution to the protein-ligand interaction energy (*i.e.*, **A1** and **A2**). The tolerances for the different sites were also readjusted using as reference more co-crystallized DPP-IV inhibitor complexes than in the original pharmacophore. The associated tolerances were thus

2.3Å for **P/D** (instead of 1.8Å), 2.0Å for **H/R1** (like in the original one), 2.5Å for **R2** (instead of 3.3Å for **H/R2**) and 1.8Å for **P/R3** (instead of 2.0Å for **H/R4**).

2.9. Protein-ligand docking and structure-based pharmacophore screening

Docking studies for the six assayed alkaloids were carried out with Glide v6.9 as follows: **(a)** the extra precision mode (*i.e.*, GlideXP) was used; **(b)** the aromatic hydrogens were considered as donors; **(c)** the maximum number of poses per ligand was increased to 32; and **(d)** the number of poses per ligand to include in the post-docking minimization was increased to 320.

Next, the docked poses of ephedrine and ephedrine-derivatives were filtered through the structure-based pharmacophore by using Phase v4.5 (Schrödinger, LLC, New York, NY, 2015) with the *score in place* option set to on (*i.e.*, no re-orientation of the docked poses was allowed during the search). Only those docked poses that matched the two compulsory sites of the structure-based pharmacophore were kept.

2.10. Lead-optimization from the (1S,2R)-(+)-norephedrine

Lead optimization was performed with CombiGlide v3.9 (Schrödinger, LLC, New York, NY, 2015) by using the *Virtual Combinatorial Screening* workflow. Initially, the phenyl group of the lowest-energy docked pose for norephedrine was replaced by a naphthyl substituent and the resulting pose for the naphthyl-containing derivative (*i.e.*, norephedrine-naph-dev) was refined with GlideXP. Then, the substituents were obtained from the Schrödinger CombiGlide Diverse Side-chain Collection v1.2 (https://www.schrodinger.com/combiglide) (which contains all reasonable ionization and tautomeric states for a collection of 817 representative functional groups commonly found in pharmaceuticals, with linkers of variable lengths).

After defining the point where the substituents were attached, we established the following parameters for a single-position docking run: **(a)** the receptor grid was the same as during the previous protein-ligand docking step; **(b)** the *apply core constraints* option was used within a maximum RMSD of 1.0Å; **(c)** the *Fully enumerated* option was selected; and **(d)** the *CombiGlide XP docking* mode was used. After this process, the resulting norephedrine-naph-dev derivatives were filtered according to their ADME properties using *Druglike* filter set. Only two violations of the following criteria were allowed for these derivatives to be considered: **(a)** molecular weight less than 500 Da; **(b)** maximum 5 hydrogen bond donors; **(c)** maximum 10 hydrogen bond acceptors; **(d)** predicted octanol/water partition coefficient (*i.e.,* logP) less than 5; **(e)** 10 or less rotatable bonds; and **(f)** 150 $Å^2$ or less Van der Waals surface area. Then, the resulting derivatives were filtered again with the same structure-based pharmacophore and conditions as above but with the exception that a third compulsory site was now required (*i.e.*, **R2**). Finally, the resulting derivatives were refined with GlideXP by using default parameters. The same process was followed again with the aim of further optimizing the derivatives

(this time, by using two different norephedrine-naph-dev derivatives as the core-containing molecules where two significantly different substituents were included during the first optimization step). All previous steps for CombiGlide were performed following the same parameters and selection criteria as the first optimization step with the exception of: **(a)** the structure-based pharmacophore, in which a fourth compulsory site (*i.e.*, **P/R3**) was now required; and **(b)** the inclusion of a prediction of the toxicity or reactivity of the resulting derivatives. Thus, the number of reactive functional groups which can lead to toxicity or reactivity was restricted to the 0-2 range by measuring the #rtvFG property with QikProp v4.6 (Schrödinger, LLC, New York, NY, 2015).

3. Results and Discussion

3.1. DPP-IV inhibitory bioactivity for selected compounds

Previous *in silico* work by our research group allowed us to predict which molecules in natural extracts with a known antidiabetic effect were DPP-IV inhibitors [17]▪ . Two of these molecules, ephedrine and pseudoephedrine, have been isolated from two *Ephedra* species (*i.e.*, *Ephedra distachya* and *Ephedra alata)* with described antidiabetic bioactivity [15,16]▪ . Another four ephedrine alkaloids (*i.e.*, norephedrine, norpseudoephedrine, N-methylephedrine and N-methylpseudoephedrine) were also predicted to be DPP-IV inhibitors [17]▪ and, although no antidiabetic activity had been reported before for the natural sources from which they were isolated, they have been identified in species that share the same genus as plants with known antidiabetic properties [8]▪ . For this reason, the six molecules were experimentally assayed to determine their bioactivity on DPP-IV and the results are shown in Figure 1 and Figure S1.

The bioactivity assay shows that all six molecules are able to inhibit DPP-IV at relatively high concentrations (*i.e.*, IC_{50} values in the 124 μM to 28.890 mM range) with a dose-response behavior (see Figure S1). Therefore, all six molecules are significantly less active as DPP-IV inhibitors than commercially available ones (*e.g.*, the IC_{50} for vildagliptin, sitagliptin, alogliptin and saxagliptin is in the 3.5 to 18 nM range). Unfortunately, these six alkaloids also inhibit DPP8 and DPP9 (see Table 1) at a concentration equivalent to its IC_{50} for DPP-IV. This absence of selectivity could be because of the similar pattern of intermolecular interactions shared by these six compounds with conserved residues in all the three enzymes (*e.g.*, the Glu205/Glu206 dyad [29]▪ and the hydrophobic residues of the S1 pocket [30]▪ ; see Figure 2). These compounds are therefore expected to present the secondary effects of the DPP8 and DPP9 inhibitors [26]▪ .

3.2. Structure-activity relationship as DPP-IV inhibitors

Figure 2 shows protein-ligand docked poses for the six assayed alkaloids and suggests how they bind to the binding site. Overall, due to the low molecular weight of the tested alkaloids (at the 151-179 Da range), only a reduced number of interactions with the DPP-IV binding site are exhibited. These are **(1)**

either one or two salt bridges (depending on the alkaloid) between the ligand amino group and the Glu205/Glu206 side chains (*i.e.*, **P/D** site of the pharmacophore; see Figure S2A); **(2)** a hydrophobic interaction between the phenyl ring and the S1 pocket (*i.e.*, **H/R1** site of the pharmacophore; see Figure S2A); and **(3)** hydrogen bonds with either Glu205, Tyr662 or Asn710.

The Glu dyad has been highly conserved throughout the DPP-IV protein family for different species [29,31]· and the interactions with these two residues have been shown to be essential for DPP-IV inhibition by single amino acid point mutations [29]· . Moreover, their relevance has been demonstrated experimentally in different structure-activity relationship (SAR) studies that show how the bioactivity of DPP-IV inhibitors is strongly influenced by: **(a)** their different capacity to form salt bridges and/or hydrogen bonds with the N-terminal recognition region (which includes the Glu dyad and Tyr662); and **(b)** the electrostatic surfaces they create in this area. For instance, SAR studies have shown that a replacement of a hydroxyl group in compound **5a** by a positively charged primary amine in compound **6a** leads to a 6-fold increase in the bioactivity (*i.e.*, from IC_{50} > 100 μM to IC_{50} = 16 μM; see Figure 3A) [32]· because it allows the formation of intermolecular salt bridges with Glu205/Glu206. Also, if the configuration of the carbon containing the positively charged amino group in sitagliptin is switched from **R** to **S**, there is a 24-fold decrease in the bioactivity of the resulting enantiomer (*i.e.*, from IC_{50} = 18 nM to IC_{50} = 440 nM; see Figure 3B) due to a reduced number of interactions with the N-terminal recognition region [33]· [a similar effect has been shown for compounds **18** and **19** in relation to their corresponding stereoisomers (*i.e.*, compounds **21** and **20**; see Figures 3C and 3D) with a 10,000-fold and 15-fold decrease in bioactivity, respectively] [34]· .

The S1 pocket is formed by the side chains of residues Tyr631, Val656, Trp659, Tyr662, Tyr666 and Val711 [18,28]· and is a rigid cavity that is also highly conserved among the DPP-IV gene family [30]· . SAR studies indicate that an aromatic ring is commonly used by non-peptidomimetic inhibitors to fill the S1 pocket optimally [19,35]· . For instance, the replacement of an *n*-butyl group (compound **89**/**7**) [36,37]· by either a phenyl substituent (compound **13** [37]·) or a 3-methylphenyl substituent (compound **90** [36]·) increases the bioactivity (from IC_{50} = 520 nM to IC_{50} = 200 nM for compound **13** and to IC_{50} = 4.6 nM for compound **90**; see Figure 3E).

Therefore, the docking poses of ephedrine and ephedrine derivatives highlight the importance of these two recognition motifs, namely salt bridge and/or hydrogen bond interactions with the N-terminal recognition region and hydrophobic interactions with the S1 pocket. The fact that the IC_{50} values for all six molecules were in the μM/mM range is also consistent with previous findings that associated these interactions with basal levels of DPP-IV inhibition [38,39]· . In this regard, three co-crystallized inhibitors [*i.e.*, valine-pyrrolidide (PDB code 1N1M), 1-methylamine-1-benzyl-cyclopentane (PDB code 2BUA) and 1-biphenyl-2-ylmethanamine (PDB code 3CCB) show that small molecules (170.25 Da, 175.27 Da and 183.25 Da, respectively) are able to inhibit DPP-IV, albeit with a low micromolar affinity (K_i = 2 μM, IC_{50} = 33 μM, and IC_{50} = 30 μM, respectively), by accomplishing interactions with only these two recognition motifs. This is also supported by virtual screening studies with fragments [38]· and low molecular

weight structures [39]▪ that found micromolar bioactivity for chemical starting points able to simultaneously bind to the S1 pocket and to the N-terminal recognition region.

A comparison of the bioactivities for the six alkaloids shows that there is a large loss of bioactivity for N-methylephedrine and N-methylpseudoephedrine relative to the other ephedrine derivatives (see Figure 1). This difference could be explained by the fact that the positively charged amine group is not able to make as many salt bridges with the Glu dyad. Thus, in the case of the N-methylephedrine and N-methylpseudoephedrine pair, the amino group corresponds to a tertiary amine (see Figures 1E and 1F), while for the norephedrine/norpseudoephedrine and for the ephedrine/pseudoephedrine pairs, a primary and a secondary amine are placed, respectively (see Figures 1A, 1B, 1C and 1D). The introduction of a primary amino group can have an impact on potency [22,40,41]▪ because it can contribute with three instead of one or two interactions. For instance, substituting the piperazine ring in compound **1** (IC_{50} = 3900 nM) with a 3-aminopiperidine in compound **2** (IC_{50} = 82 nM) leads to a 48-fold gain in bioactivity (see Figure 3F) [42]▪ . Unfortunately, the docked poses for the six compounds do not allow us to explain their bioactivity differences. For instance, although the bioactivity of ephedrine and norephedrine are higher than their corresponding pseudo partners, their docked poses show no differences in terms of their intermolecular interactions with the DPP-IV binding site. Likewise, the intermolecular interactions of the docked poses for norephedrine and N-methylephedrine are not sufficiently different (see Figures 1C and 1E) to explain the differences in bioactivity between the two compounds.

3.3. Using norephedrine as a lead compound for computationally designing new DPP-IV inhibitors

Our results show that ephedrine derivatives have a basal DPP-IV inhibitory activity and, consequently, that these natural products are interesting to medicinal chemistry as promising lead compounds for designing potent and selective DPP-IV inhibitors. In our case, we have selected norephedrine for performing such computational drug design. Moreover, it should be necessary to consider how to decrease the cardiovascular side effects associated with the activation of adrenergic receptors by the resulting norephedrine derivatives. In that sense, the first aim was to develop an antagonist (*i.e.*, a β-blocker) via appropriate chemical modifications of norephedrine. It has been reported that adrenergic receptor agonists promote conformational changes at the binding site of the β_1 and β_2 adrenergic receptors by interacting with two Ser residues. In contrast, β-blockers do not make polar interactions with both Ser residues and, therefore, do not promote the above mentioned conformational changes [43]▪ . Consequently, the reduction of polar interaction with both Ser residues and, instead, the promotion of hydrophobic interactions with them has been suggested to stimulate antagonist binding [43]▪ . For instance, the replacement of the catechol ring of isoprenaline by a phenyl ring at 2-(isopropylamino)-1-phenylethanol reduces the agonist activity whereas the replacement by a naphthalene ring yield to pronethalol, the first clinical candidate as β-blocker (see Figure S3). Therefore, following this schema, the first step on using norephedrine as a lead molecule for the design of new DPP-IV inhibitors was the substitution of its phenyl by a naphthyl ring (see Figure 4A). This is

not only expected to avoid the agonistic behavior of further norephedrine derivatives but also to promote antagonistic effects and increase the occupancy of the S1 pocket (which is expected to increase the bioactivity of the resulting derivatives as DPP-IV inhibitors [36]▪).

With the aim of improving the binding affinity and the selectivity for DPP-IV, we have used as the starting point for lead optimization the lowest-energy docked pose of norephedrine-naph-dev (with a GlideXP GScore of -9.061 kcal/mol; see Figure 4A). In this sense, the optimization process has been designed with the goal of building norephedrine-naph-dev derivatives that reach the S2 extensive subsite of DPP-IV (*i.e.*, the **R2** site of the pharmacophore) and interact with Tyr547 of DPP-IV (*i.e.*, the **P/R3** site of the pharmacophore).

The reason for this selection is that π-π stacking intermolecular interaction between the ligand and Phe357 (one of the residues of the S2 extensive subsite) has recently been demonstrated to increase bioactivity and selectivity in DPP-IV inhibitors [22,44]▪ . For instance, compounds **25**, **31** and **42** (co-crystallized with DPP-IV at the PDB structures encoded as 2I78, 2OQI and 2OQV; respectively) were developed in a lead optimization process from a low MW compound (*i.e.*, **6** with 207.70 Da; see Figure 3G) [45]▪ . Thus, the corresponding SAR studies show how compound **6** (K_i = 0.82 μM) can be modified to become compounds **25**, **31** and **42** for reaching the S2 extensive subsite by establishing either hydrophobic or π-π interactions that lower K_i to the 1.3-4.0 nM range for DPP-IV. Another example is compound **22e** [46]▪ , whose π-π interaction between its indolinyl moiety and Phe357 improves 116-fold its bioactivity relative to compound **10** (which has the same structure as **22e** with the exception that in **10**, no substituent fills the S2 extensive subsite because **10** lacks a substituent equivalent to the indolinyl moiety in **22e**; see Figure 3H) [46]▪ . Moreover, as previously mentioned, the S2 extensive subsite has been described as governing the selectivity for DPP-IV over DPP8 and DPP9 [22,23]▪ . For these reasons, a point of attachment was placed on the methyl group of the lead (see the **R** label at Figure 4A) with the aim of establishing π-π intermolecular stacking with Phe357. Therefore, only derivatives that met all the following criteria were selected: **(a)** reaching the **R2** site at the pharmacophore; **(b)** making the π-π interaction with Phe357; and **(c)** being drug-like with proper ADME properties. The resulting derivatives were then visually inspected and only those with significantly different substituents (*i.e.*, norephedrine-naph-dev-199 and norephedrine-naph-dev-443) were considered for further optimization (see Figures 4B and 4C).

Next, a second optimization step was performed using norephedrine-naph-dev-199 and norephedrine-naph-dev-443 (see Figures 4B and 4C) with the aim of establishing either additional π-π stacking or cation-π interactions with Tyr547 (a residue that plays a major role stabilizing the oxyanion intermediate and is essential for the cleavage of the prolyl peptide bond of the substrate) [47,48]▪ . This step was taken because interactions with Tyr547 have been described as improving the potency of DPP-IV inhibitors [22]▪ and as possibly increasing the ligand's selectivity [49]▪ . For instance, the uracil ring of alogliptin and trelagliptin and the xanthine ring of linagliptin are able to form π-π stacking interactions with Tyr547 to contribute to the inhibitory potency of these drugs (*i.e.*, 9 nM, 4.2 nM and 1 nM,

respectively). In order to achieve the intermolecular interaction with Tyr547, another attachment point was then defined for each lead (see the **R1** and **R2** label at Figures 4B and 4C). Finally, only derivatives that met all the following criteria were considered: **(a)** reaching the **R3** site of the pharmacophore; **(b)** making π-π or cation-π interactions with Tyr547; **(c)** being drug-like with proper ADME/Tox properties; and **(d)** having a better XP GScore than the lead compounds. The derivatives that met all these criteria are shown in Tables 2 and 3 and the docked pose for the best derivative at each attachment point is shown in Figure 5.

Remarkably, the XP GScores for these norephedrine-derivatives increased to -12.520 kcal/mol, which is even higher than the XP GScore obtained for crystallized gliptins such as alogliptin, sitagliptin, linagliptin and anagliptin (from -8.096 to -10.833 kcal/mol; see Table S2). The norephedrine-derivatives maintain the most important protein-ligand interactions found in the norephedrine core for a basal inhibitory activity of DPP-IV. Additionally, all of them are able to reproduce most of the important intermolecular interactions described in previous SAR studies (*i.e.,* S2 extensive subsite and Tyr547) for increasing binding affinity and selectivity for DPP-IV and they are therefore likely to exhibit nanomolar activity as inhibitors.

4. Conclusion

The World Health Organization and the International Diabetes Federation have reported that between 340 and 536 million people worldwide currently have diabetes and it is forecast that diabetes deaths will double between 2005 and 2030, thus making it the 7th leading cause of death by 2030. Moreover, the use of several natural products (with different *Ephedra* herbs among them) has been reported as useful for reducing and preventing hyperglycemia [1,2,4]▪ . The results of the present study experimentally demonstrated that among the antidiabetic properties previously described for *Ephedra* species [15,16]▪ at least one of the mechanisms is the inhibition of DPP-IV by some of the alkaloids found in their extracts. In this regard, it has been suggested that ephedrine and pseudoephedrine account for nearly 99% of total alkaloids in some *Ephedra* species [8]▪ . Unfortunately, several adverse effects have been described for ephedrine and ephedrine-derivatives and, as a consequence, their use has been severely restricted as food supplements by the EFSA and the FDA [14]▪ . Nevertheless, we have shown here how their basal activity as DPP-IV inhibitors could be taken advantage of to design derivatives that, according to well-established computational approaches and SAR studies, would have proper ADME/Tox properties, improved potency and selectivity as antidiabetics and with low agonist activity for adrenergic receptors.

5. Future perspective

Recent clinical trials reported a possible cardioprotective effect of the DPP-IV inhibitors beyond the glycemic control. However, the molecular mechanism whereby these inhibitors improves cardiovascular metabolism remains unclear and further studies are needed to determine the underlying benefits. Our

study reports a link between DPP-IV and β-adrenergic receptors throughout ephedrine and ephedrine-derivatives that bind to both kind of targets and, therefore, this opens the door to design potent and selective DPP-IV inhibitors that have also β-blocker activity. At this point, it is worth to remind that this is not the first time that this is suggested. Thus, Li & Yang patented a series of DPP-IV inhibitors that were claimed by the authors to show also bioactivity as β-blockers [50]▪ . Unfortunately, Li & Yang do not explain how they find the connection between DPP-IV and β-adrenergic receptors but described the molecules they patented as useful in the treatment of neurological disorders, diabetes, inflammatory disorders such as arthritis, obesity, osteoporosis, hypertension and glaucoma. Therefore, the alkaloids of *Ephedra* are promising lead structures to develop new antidiabetic drugs with additional cardiovascular benefits as β-blockers.

Finally, preliminary studies in our lab have found that some of the β-blockers approved by the health agencies show bioactivity as DPP-IV inhibitors and we are also comparing the binding sites of both targets type in order to understand how: **(a)** this dual bioactivity is achieved; and **(b)** to optimize the structure of lead molecules to simultaneously obtain high bioactivities for a single molecule. In our opinion, the results of this research will have a great impact on the treatment of the metabolic syndrome.

6. Executive summary

- *Ephedra* alkaloids bioactivities are evaluated *in vitro* due to their predicted antidiabetic properties as DPP-IV inhibitors.
- These compounds are experimentally confirmed to be DPP-IV inhibitors, exhibiting inhibitory activities ranged from 124 μM to 28.890 mM.
- The intermolecular interactions with DPP-IV are described by protein-ligand docking.
- These alkaloids are able to interact with the N-terminal recognition motif and the S1 pocket, both considered to be the most important anchor points for DPP-IV inhibitor recognition.
- Norephedrine is used as a lead compound to computationally suggest how to design new potent and selective DPP-IV inhibitors with low agonist activity for adrenergic receptors.
- A link between DPP-IV and β-adrenergic receptors throughout *Ephedra* alkaloids has been established and, therefore, this opens the door to design potent and selective DPP-IV inhibitors with β-blocker activity.

Figure 1. Percentage of DPP-IV activity relative to the concentration (in M) for each assayed compound. DPP-IV inhibitory dose-response curve was obtained via a competitive binding assay. The data represent the mean ± SD of an experiment performed in triplicate. A non-linear regression (curve fit) followed by sigmoidal dose-response curve (variable slope) was made to find the IC_{50}. Each panel includes also the 2D structure of the ionization state of the corresponding molecule at pH 7.

Figure 2. The best docked poses (with the corresponding XP GScore) for the six studied *Ephedra* alkaloids at the DPP-IV binding site. Blue dashed lines show π-π stacking intermolecular interactions whereas the red ones show either salt bridges (between the positively charged amine and the Glu dyad) or hydrogen bonds. All panels have the same orientation to allow easy comparison between them.

Figure 3. Chemical structures from SAR studies that are discussed in this paper. Compounds in the same panel show important changes in their DPP-IV bioactivity as a consequence of localized changes in their structures (highlighted with a red line surrounding them). Compounds in each panel are classified by increasing bioactivity from left to right.

Figure 4. Lead optimization of norephedrine-naph-dev that aims to obtain derivatives with improved potency and selectivity for DPP-IV. Firstly, a substituent was attached to the methyl substituent (see Figure 4A) in order to reach the S2 extensive subsite (*i.e.,* the **R2** site at the pharmacophore) and allow a π-π stacking interaction with Phe357. As a result of the first optimization and the application of the corresponding selection criteria, two derivatives (*i.e.*, norephedrine-naph-dev-199 and norephedrine-naph-dev-443) were selected for further optimization (see Figures 4B and 4C, respectively). Furthermore, another point for the attachment of new substituents was also selected on each derivative in order to allow either cation-π or π-π stacking interactions with Tyr547 (reaching the **P**/**R3** site of the pharmacophore). Names for the derivatives obtained after this second optimization step are classified according to the attachment position and sorted by their XP GScore (see also their 2D structure and XP GScore at Tables 2 and 3).

Figure 5. Lowest-energy docked poses of the derivatives obtained after second optimization step. The coordinates for DPP-IV that were used during the docking correspond to the PDB file with code 1X70. Blue dashed lines show either π-cation or π-π stacking intermolecular interactions whereas the red ones show either salt bridges (between the positively charged amine and the Glu dyad) or hydrogen bonds. All panels have the same orientation to allow easy comparison between them.

Table 1. Bioactivity data of the *Ephedra* alkaloids on DPP-IV, DPP8 and DPP9.

IC_{50} has been calculated for DPP-IV, whereas for DPP8 and DPP9 the value corresponds to the percentage of inhibition using a concentration of each compound equivalent to its IC_{50} for DPP-IV.

Table 2. Best norephedrine-naph-dev-199 derivatives obtained in the second optimization step.

Molecules are sorted according to XP GScore. The name for each derivative was built by adding the code of the attached fragment (according to the CombiGlide Diverse Side-chain Collection) to the lead name.

Table 3. Best norephedrine-naph-dev-443 derivatives obtained in the second optimization step.

Molecules are sorted according to XP GScore. The name for each derivative was built by adding the code of the attached fragment (according to the CombiGlide Diverse Side-chain Collection) to the lead name.

References

1. Patel DK, Prasad SK, Kumar R, Hemalatha S. An overview on antidiabetic medicinal plants having insulin mimetic property. *Asian Pac. J. Trop. Biomed.* 2(4), 320–30 (2012).

2. Rizvi SI, Mishra N. Traditional Indian medicines used for the management of diabetes mellitus. *J. Diabetes Res.* 2013, 712092 (2013).

3. Newman DJ, Cragg GM. Natural products as sources of new drugs over the 30 years from 1981 to 2010. *J. Nat. Prod.* 75(3), 311–35 (2012).

4. Chauhan A, Sharma PK, Srivastava P, Kumar N, Dudhe R. Plants having potential antidiabetic activity: a review. *Der Pharm. Lett.* 2(3), 369–387 (2010).

5. Lee MR. The history of *Ephedra* (ma-huang). *J. R. Coll. Physicians Edinb.* 41(1), 78–84 (2011).

6. Mahdihassan S, Mehdi FS. Soma of the Rigveda and an attempt to identify it. *Am. J. Chin. Med.* 17(01n02), 1–8 (1989).

7. Abourashed EA, El-Alfy AT, Khan IA, Walker L. *Ephedra* in perspective – a current review. *Phytother. Res.* 17(7), 703–12 (2003).

8. Ibragic S, Sofic E. Chemical composition of various *Ephedra* species. *Bosn. J. Basic Med. Sci.* 15(3), 21–7 (2015).

9. Stohs SJ, Badmaev V. A review of natural stimulant and non-stimulant thermogenic agents. *Phyther. Res.* 30(5), 732–40 (2016).

10. Gurley BJ, Steelman SC, Thomas SL. Multi-ingredient, caffeine-containing dietary supplements: history, safety, and efficacy. *Clin. Ther.* 37(2), 275–301 (2015).

11. Solanki P, Yadav P, Kantharia N. Ephedrine: direct, indirect or mixed acting sympathomimetic? *Int. J. Basic Clin. Pharmacol.* 3(3), 431 (2014).

12. Stoynova V, Getov I. Review of the drug safety profile and prescription regulations of medicinal products containing ephedrine and pseudoephedrine. *J. Clin. Med.* 3(3), 41–50 (2010).

13. Fleming RM. Safety of *Ephedra* and related anorexic medications. *Expert Opin. Drug Saf.* 7(6), 749–59 (2008).

14. EFSA ANS Panel (EFSA Panel on Food Additives and Nutrient Sources). Scientific opinion on safety evaluation of *Ephedra* species for use in food. *EFSA J.* 11(11), 3467 (2013).

15. Shabana MM, Mirhom YW, Genenah AA, Aboutabl EA, Amer HA. Study into wild Egyptian plants of potential medicinal activity. Ninth communication: hypoglycaemic activity of some selected plants in normal fasting and alloxanised rats. *Arch. Exp. Veterinarmed.* 44(3), 389–94 (1990).

16. Xiu LM, Miura AB, Yamamoto K, *et al.* Pancreatic islet regeneration by ephedrine in mice with streptozotocin-induced diabetes. *Am. J. Chin. Med.* 29(3-4), 493–500 (2001).

*** Experimental design showing that Ephedra extract promoted the regeneration of pancreas islets and restore the secretion of insulin.**

17. Guasch L, Sala E, Ojeda MJ, *et al.* Identification of novel human dipeptidyl peptidase-IV inhibitors of natural origin (part II): *in silico* prediction in antidiabetic extracts. *PLoS One*. 7(9), e44972 (2012).

**** Previous computational study that predicted ephedrine and pseudoephedrine as potential DPP-IV inhibitors.**

18. Ojeda MJ, Cereto-Massagué A, Valls C, Pujadas G. DPP-IV, an important target for antidiabetic functional food design. in: Foodinformatics, applications of chemical information to food chemistry, *Springer*, 177-212 (2014).

19. Costante R, Stefanucci A, Carradori S, Novellino E, Mollica A. DPP-4 inhibitors: a patent review (2012 - 2014). *Expert Opin. Ther. Pat.* 25(2), 209–36 (2015).

20. Kwok AJ, Mashar M, Khavandi K, Sabir I. DPP-IV inhibitors: Beyond glycaemic control? *Trends Cardiovasc. Med.* 24(4), 157–64 (2014).

21. Opinto G, Natalicchio A, Marchetti P. Physiology of incretins and loss of incretin effect in type 2 diabetes and obesity. *Arch. Physiol. Biochem.* 119(4), 170–8 (2013).

22. Patel BD, Ghate MD. Recent approaches to medicinal chemistry and therapeutic potential of dipeptidyl peptidase-4 (DPP-4) inhibitors. *Eur. J. Med. Chem.* 74, 574–605 (2014).

23. Smelcerovic A, Miljkovic F, Kolarevic A, *et al.* An overview of recent dipeptidyl peptidase-IV inhibitors: linking their structure and physico-chemical properties with SAR, pharmacokinetics and toxicity. *Curr. Top. Med. Chem.* 15(23), 2342–72 (2015).

*** Recent review on natural and synthetic DPP-IV inhibitors, focusing on the association between their chemical structure and mechanism of action.**

24. Shirakawa J, Amo K, Ohminami H, *et al.* Protective effects of dipeptidyl peptidase-4 (DPP-4) inhibitor against increased β cell apoptosis induced by dietary sucrose and linoleic acid in mice with diabetes. *J. Biol. Chem.* 286(29), 25467–76 (2011).

25. Mega C, Vala H, Rodrigues-Santos P, *et al.* Sitagliptin prevents aggravation of endocrine and exocrine pancreatic damage in the Zucker Diabetic Fatty rat - focus on amelioration of metabolic profile and tissue cytoprotective properties. *Diabetol. Metab. Syndr.* 6(1), 42 (2014).

26. Lankas GR, Leiting B, Roy RS, *et al.* Dipeptidyl peptidase IV inhibition for the treatment of type 2 diabetes: potential importance of selectivity over dipeptidyl peptidases 8 and 9. *Diabetes*. 54(10), 2988–94 (2005).

27. Cereto-Massagué A, Ojeda MJ, Joosten RP, *et al.* The good, the bad and the dubious: VHELIBS, a validation helper for ligands and binding sites. *J. Cheminform.* 5(1), 36 (2013).

28. Guasch L, Ojeda MJ, González-Abuín N, *et al.* Identification of novel human dipeptidyl peptidase-IV inhibitors of natural origin (part I): Virtual screening and activity assays. *PLoS One*. 7(9), e44971 (2012).

29. Abbott CA, McCaughan GW, Gorrell MD. Two highly conserved glutamic acid residues in the

predicted β propeller domain of dipeptidyl peptidase IV are required for its enzyme activity. *FEBS Lett.* 458(3), 278–84 (1999).

30. Pitman MR, Menz RI, Abbott CA. Hydrophilic residues surrounding the S1 and S2 pockets contribute to dimerisation and catalysis in human dipeptidyl peptidase 8 (DP8). *Biol. Chem.* 391(8), 959–72 (2010).

31. Ajami K, Abbott CA, Obradovic M, *et al.* Structural requirements for catalysis, expression, and dimerization in the CD26/DPIV gene family. *Biochemistry*. 42(3), 694–701 (2003).

32. Banno Y, Miyamoto Y, Sasaki M, *et al.* Identification of 3-aminomethyl-1,2-dihydro-4-phenyl-1-isoquinolones: a new class of potent, selective, and orally active non-peptide dipeptidyl peptidase IV inhibitors that form a unique interaction with Lys554. *Bioorg. Med. Chem.* 19(16), 4953–70 (2011).

33. Kim D, Wang L, Beconi M, *et al.* (2*R*)-4-oxo-4-[3-(trifluoromethyl)-5,6-dihydro[1,2,4]triazolo[4,3-a]pyrazin-7(8*H*)-yl]-1-(2,4,5-trifluorophenyl)butan-2-amine: a potent, orally active dipeptidyl peptidase IV inhibitor for the treatment of type 2 diabetes. *J. Med. Chem.* 48(1), 141–51 (2005).

34. Biftu T, Feng D, Qian X, *et al.* (3R)-4-[(3R)-3-Amino-4-(2,4,5-trifluorophenyl)butanoyl]-3-(2,2,2-trifluoroethyl)-1,4-diazepan-2-one, a selective dipeptidyl peptidase IV inhibitor for the treatment of type 2 diabetes. *Bioorg. Med. Chem. Lett.* 17(1), 49–52 (2007).

35. Li Q, Zhou M, Han L, *et al.* Design, synthesis and biological evaluation of imidazo[1,2-a]pyridine derivatives as novel DPP-4 inhibitors. *Chem. Biol. Drug Des.* 86(4), 849–56 (2015).

36. Liu Y, Hu Y, Liu T. Recent advances in non-peptidomimetic dipeptidyl peptidase 4 inhibitors: Medicinal chemistry and preclinical aspects. *Curr. Med. Chem.* 19(23), 3982–99 (2012).

37. Lübbers T, Böhringer M, Gobbi L, *et al.* 1,3-disubstituted 4-aminopiperidines as useful tools in the optimization of the 2-aminobenzo[a]quinolizine dipeptidyl peptidase IV inhibitors. *Bioorg. Med. Chem. Lett.* 17(11), 2966–70 (2007).

38. Rummey C, Nordhoff S, Thiemann M, Metz G. *In silico* fragment-based discovery of DPP-IV S1 pocket binders. *Bioorg. Med. Chem. Lett.* 16(5), 1405–9 (2006).

39. Ward RA, Perkins TDJ, Stafford J. Structure-based virtual screening for low molecular weight chemical starting points for dipeptidyl peptidase IV inhibitors. *J. Med. Chem.* 48(22), 6991–6 (2005).

40. Gaba M, Singh S, Gaba P. Dipeptidyl peptidase-4 inhibitors: a new approach in diabetes treatment. *Int. J. drug Dev. Res.* 1(1), 146–156 (2009).

41. Villhauer EB, Brinkman JA, Naderi GB, *et al.* 1-[[(3-hydroxy-1-adamantyl)amino]acetyl]-2-cyano-(S)-pyrrolidine: a potent, selective, and orally bioavailable dipeptidyl peptidase IV inhibitor with antihyperglycemic properties. *J. Med. Chem.* 46(13), 2774–89 (2003).

42. Schnapp G, Klein T, Hoevels Y, Bakker RA, Nar H. Comparative analysis of binding kinetics and thermodynamics of dipeptidyl peptidase-4 inhibitors and their relationship to structure. *J. Med. Chem.* 59(16), 7466–7477 (2016).

43. Chan HCS, Filipek S, Yuan S. The principles of ligand specificity on β-2-adrenergic receptor. *Sci. Rep.* 6(1), 34736 (2016).

44. Rummey C, Metz G. Homology models of dipeptidyl peptidases 8 and 9 with a focus on loop predictions near the active site. *Proteins*. 66(1), 160–71 (2007).

45. Pei Z, Li X, von Geldern TW, *et al.* Discovery of ((4R,5S)-5-amino-4-(2,4,5- trifluorophenyl)cyclohex-1-enyl)-(3- (trifluoromethyl)-5,6-dihydro- [1,2,4]triazolo[4,3-a]pyrazin-7(8H)-yl)methanone (ABT-341), a highly potent, selective, orally efficacious, and safe dipeptidyl peptidase IV inhibi. *J. Med. Chem.* 49(22), 6439–42 (2006).

46. Sakashita H, Akahoshi F, Yoshida T, *et al.* Lead optimization of [(S)-γ-(arylamino)prolyl]thiazolidine focused on γ-substituent: Indoline compounds as potent DPP-IV inhibitors. *Bioorg. Med. Chem.* 15(2), 641–55 (2007).

47. Bjelke JR, Christensen J, Branner S, *et al.* Tyrosine 547 constitutes an essential part of the catalytic mechanism of dipeptidyl peptidase IV. *J. Biol. Chem.* 279(33), 34691–7 (2004).

48. Metzler WJ, Yanchunas J, Weigelt C, *et al.* Involvement of DPP-IV catalytic residues in enzyme-saxagliptin complex formation. *Protein Sci.* 17(2), 240–50 (2008).

49. Longenecker KL, Stewart KD, Madar DJ, *et al.* Crystal structures of DPP-IV (CD26) from rat kidney exhibit flexible accommodation of peptidase-selective inhibitors. *Biochemistry*. 45(24), 7474–82 (2006).

50. Li W, Yang C. US20130184322 A1- Novel Dipeptidyl-Peptidase-IV inhibitors. (2013).

**** The first time that some molecules are described, simultaneously, as DPP-IV inhibitors and β-blockers.**

Figure 1

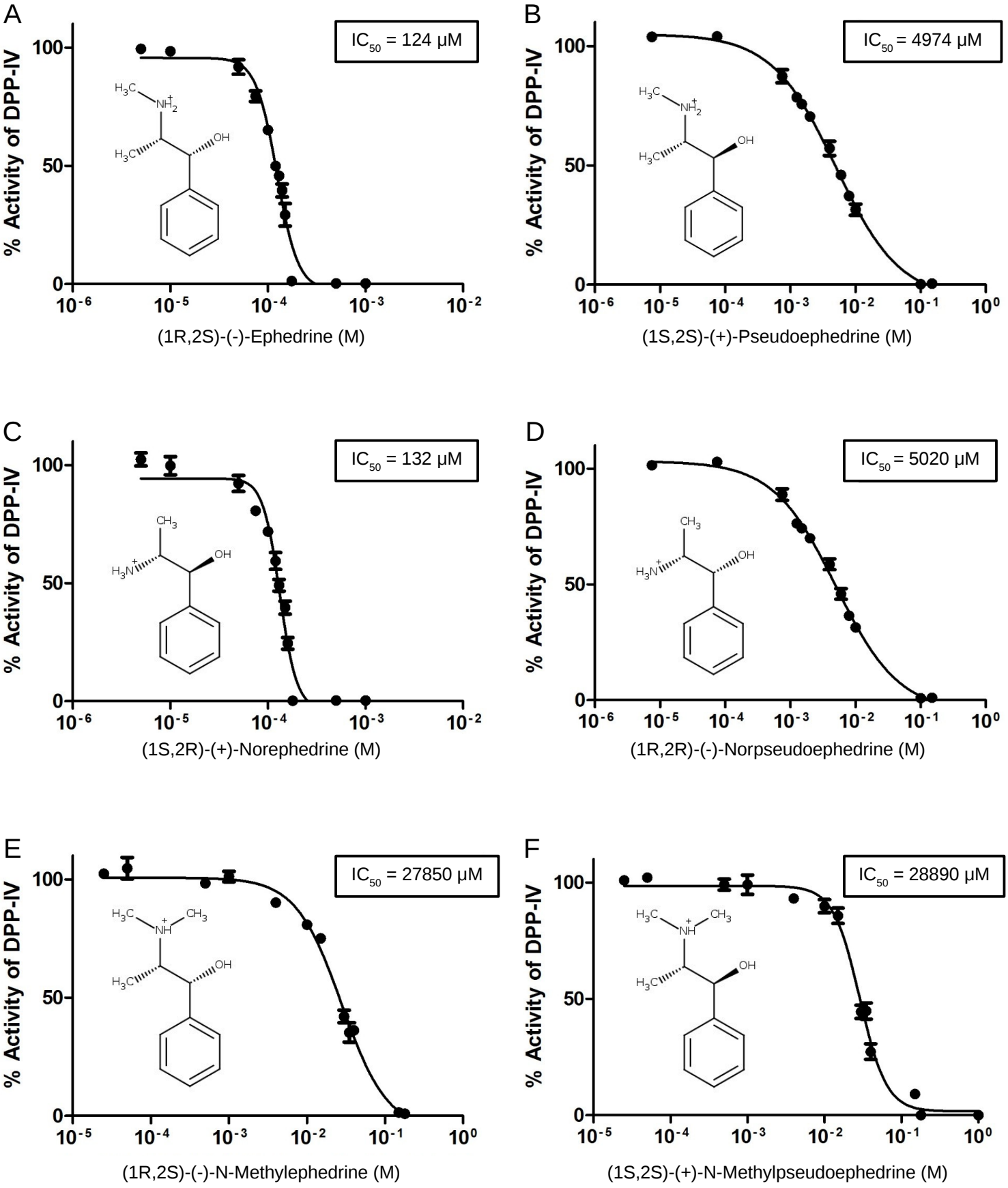
A
IC50 = 124 µM
% Activity of DPP-IV
(1R,2S)-(-)-Ephedrine (M)
B
IC50 = 4974 µM
% Activity of DPP-IV
(1S,2S)-(+)-Pseudoephedrine (M)
C
IC50 = 132 µM
% Activity of DPP-IV
(1S,2R)-(+)-Norephedrine (M)
D
IC50 = 5020 µM
% Activity of DPP-IV
(1R,2R)-(-)-Norpseudoephedrine (M)
E
IC50 = 27850 µM
% Activity of DPP-IV
(1R,2S)-(-)-N-Methylephedrine (M)
F
IC50 = 28890 µM
% Activity of DPP-IV
(1S,2S)-(+)-N-Methylpseudoephedrine (M)

Figure 2

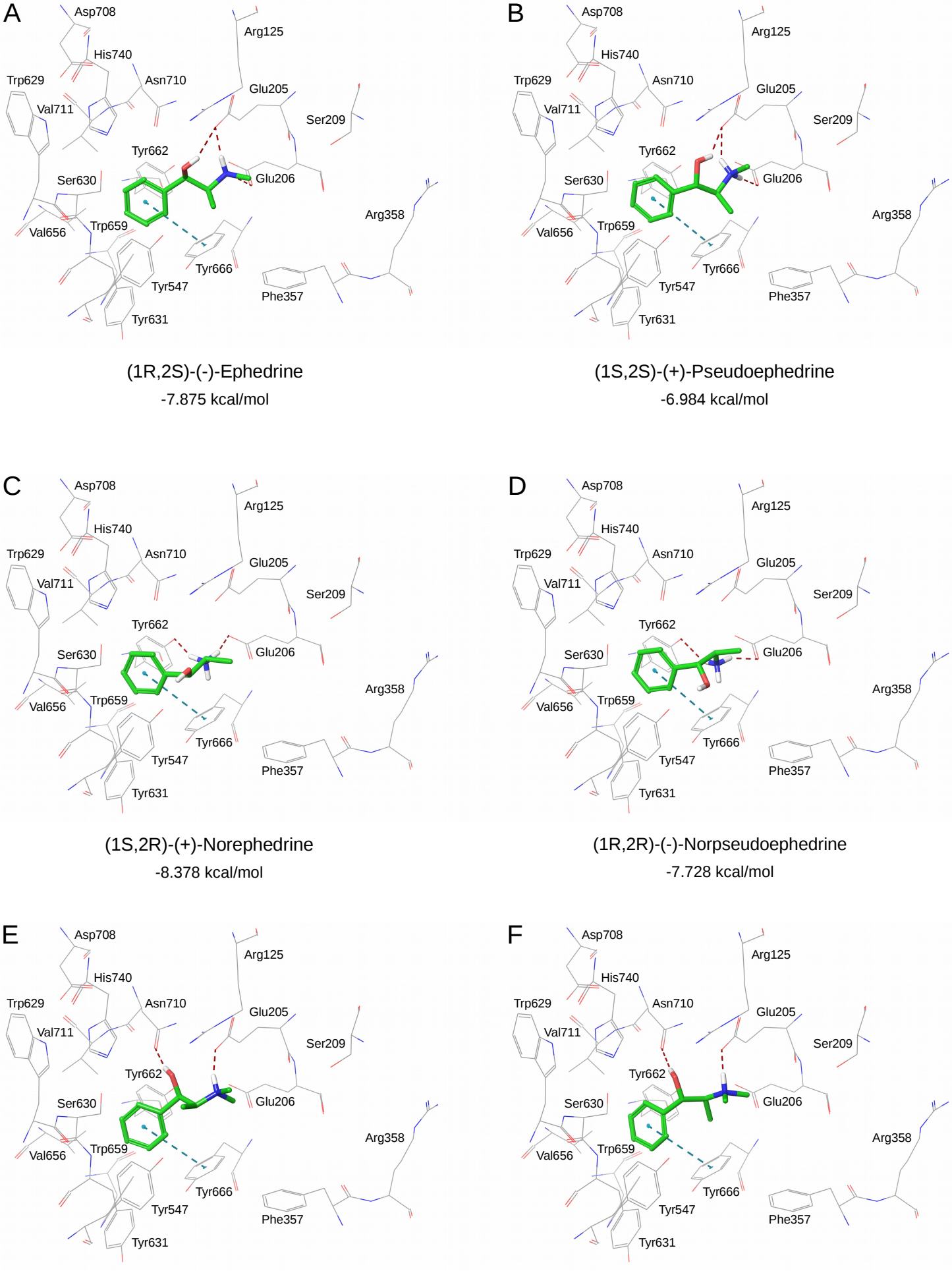

(1R,2S)-(-)-Ephedrine

-7.875 kcal/mol

(1S,2S)-(+)-Pseudoephedrine

-6.984 kcal/mol

(1S,2R)-(+)-Norephedrine

-8.378 kcal/mol

(1R,2R)-(-)-Norpseudoephedrine

-7.728 kcal/mol

(1R,2S)-(-)-N-Methylephedrine

-6.139 kcal/mol

(1S,2S)-(+)-N-Methylpseudoephedrine

-5.585 kcal/mol

Figure 3

A

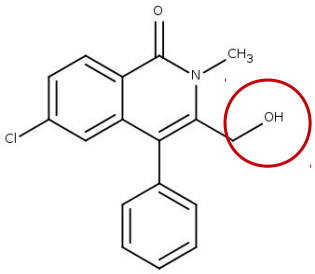

5a [32]
IC_{50} > 100 μM

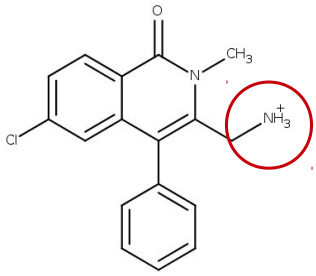

6a [32]
IC_{50} = 16 μM

B

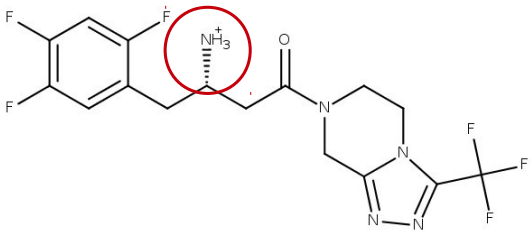

(S)-Sitagliptin [33]
IC_{50} = 440 nM

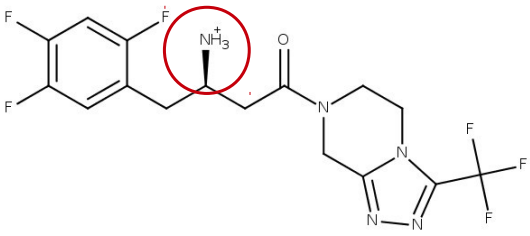

(R)-Sitagliptin [33]
IC_{50} = 18 nM

C

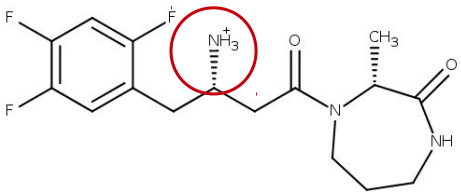

21 [34]
IC_{50} = 67000 nM

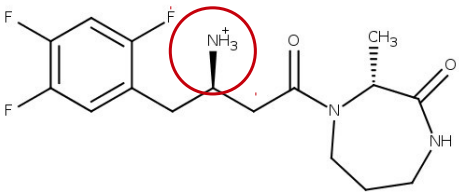

18 [34]
IC_{50} = 6.6 nM

D

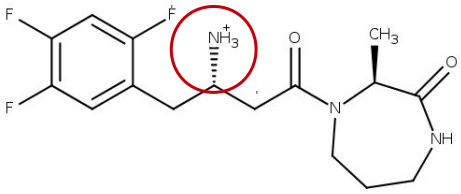

20 [34]
IC_{50} = 2300 nM

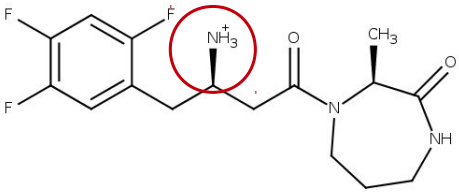

19 [34]
IC_{50} = 150 nM

E

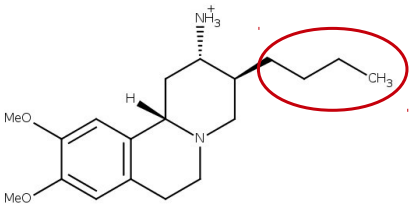

89/7 [36,37]
IC_{50} = 520 nM

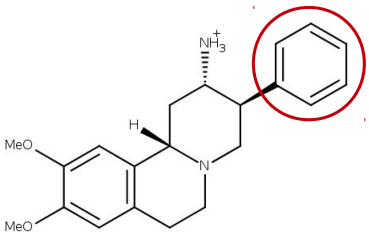

13 [37]
IC_{50} = 200 nM

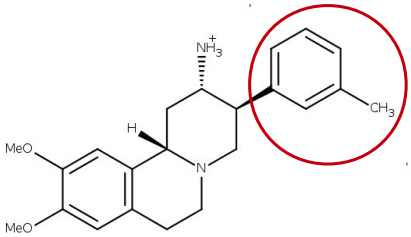

90 [36]
IC_{50} = 4.6 nM

F

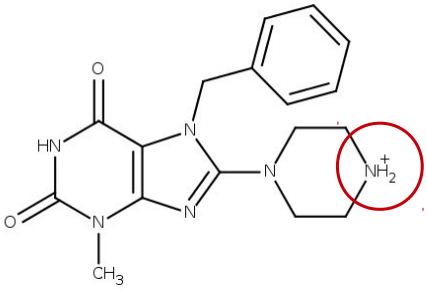

1 [42]
IC_{50} =3900 nM

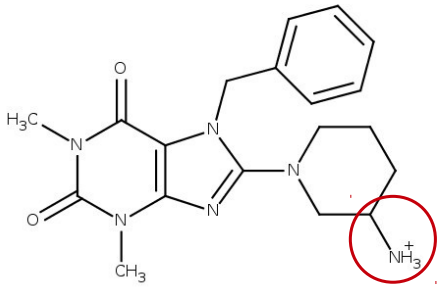

2 [42]
IC_{50} = 82 nM

G

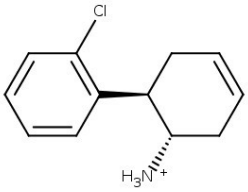

6 [45]
K_i = 0.82 μM

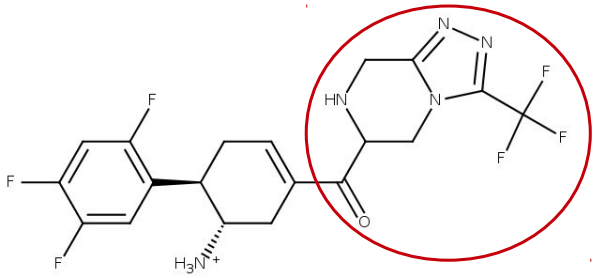

25 (PDB code 2I78)
K_i = 1.3 nM

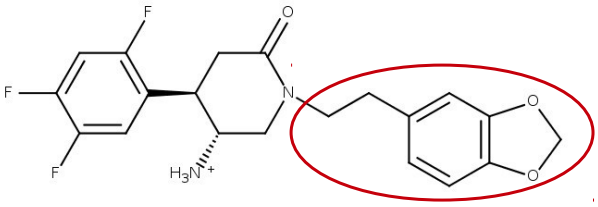

31 (PDB code 2OQI)
K_i = 3.2 nM

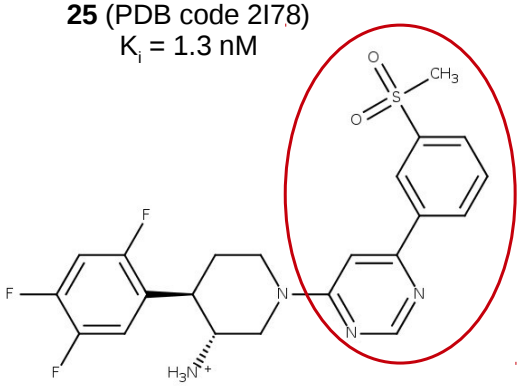

42 (PDB code 2OQV)
K_i = 4.0 nM

H

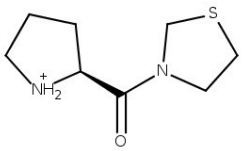

10 [46]
IC_{50} = 538 nM

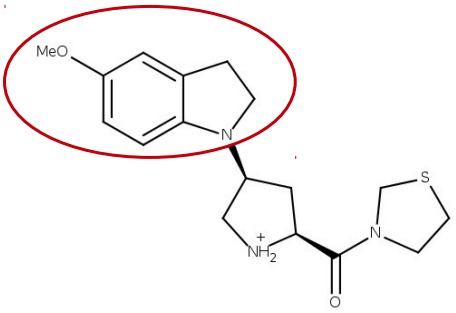

22e [46]
IC_{50} = 4.8 nM

Figure 4

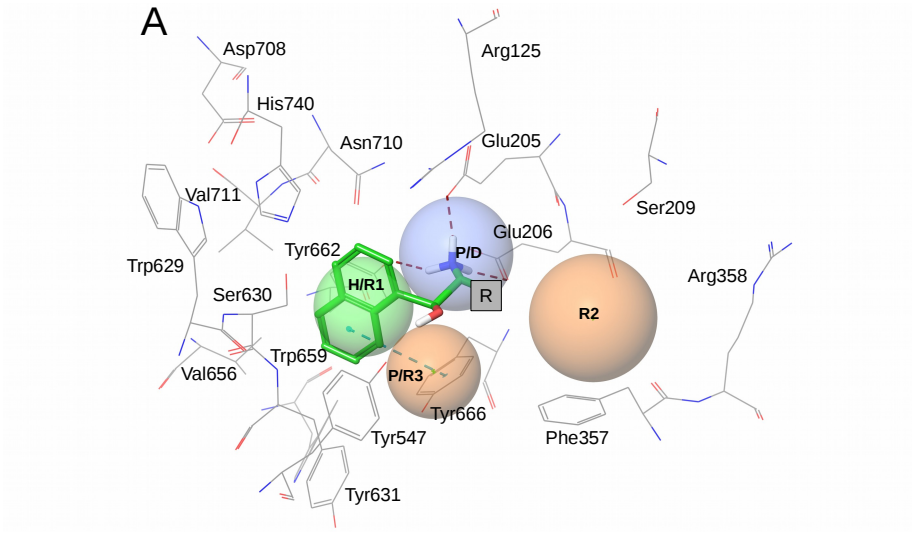

Norephedrine-naph-dev

-9.061 kcal/mol

FIRST OPTIMIZATION STEP

Only candidates that simultaneously:

- accomplish the **R2** site of the pharmacophore
- make π-π interaction with Phe357
- are drug-like with proper ADME properties
- include significantly different substituents

are further optimized

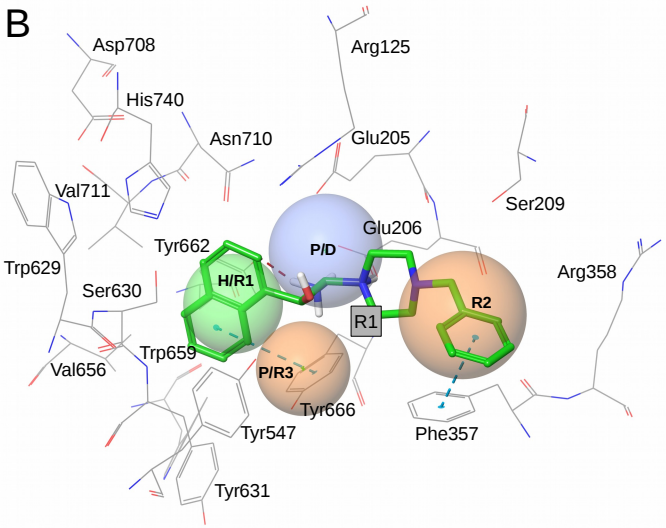

Norephedrine-naph-dev-199

-11.194 kcal/mol

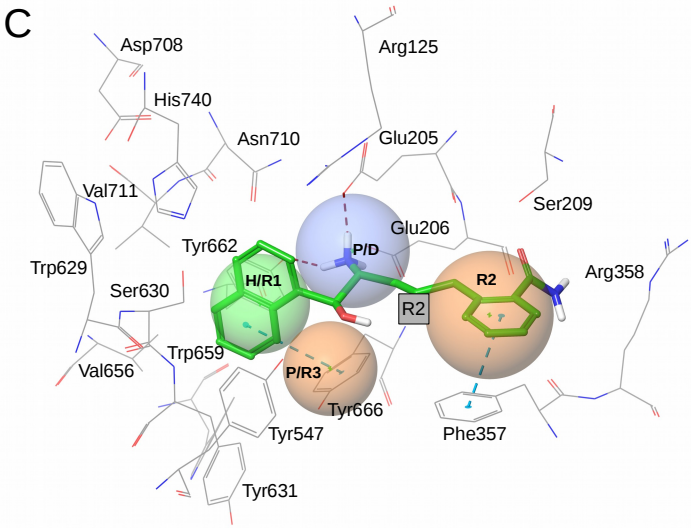

Norephedrine-naph-dev-443

-11.069 kcal/mol

SECOND OPTIMIZATION STEP

Only candidates that simultaneously:

- accomplish the **P/R3** site of the pharmacophore
- make π-π or cation-π interaction with Tyr547
- are drug-like with proper ADME/Tox properties
- have a XP GScore more negative than the leads

Norephedrine-naph-dev-199 derivatives
R1
199-279
199-701
199-303
199-93

Norephedrine-naph-dev-443 derivatives
R2
443-182
443-177

Figure 5

A

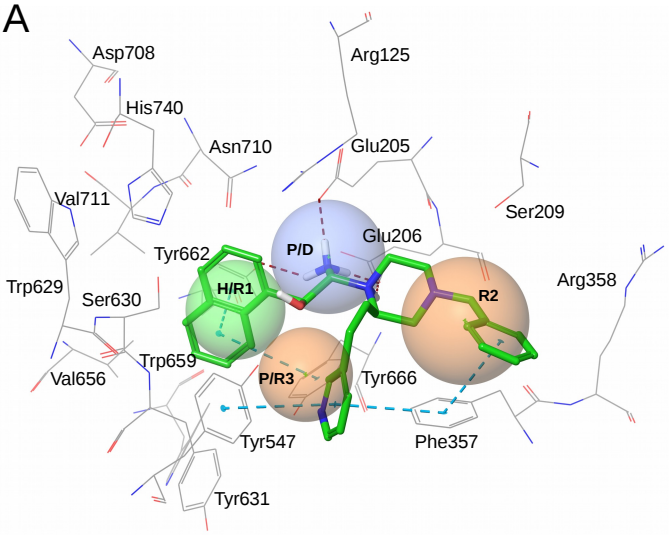

Norephedrine-naph-dev-199-279

-12.520 kcal/mol

B

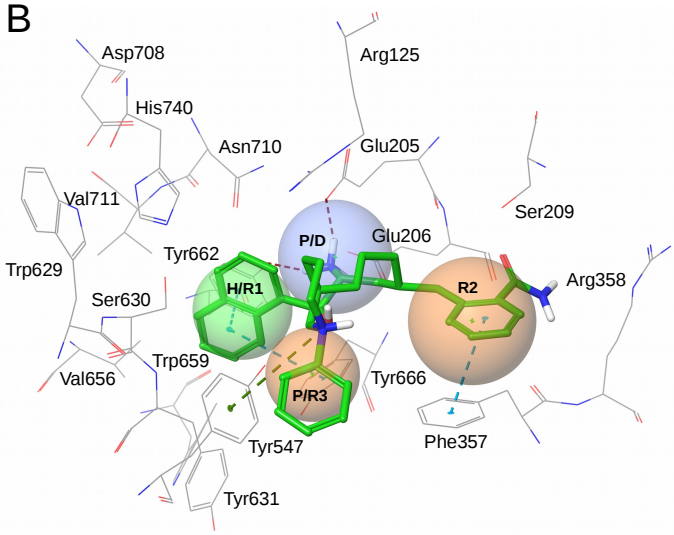

Norephedrine-naph-dev-443-182

-11.763 kcal/mol

Table 1

Ephedra alkaloid	DPP-IV IC_{50} (μM)	% of inhibition for DPP8 (% ± SD)	% of inhibition for DPP9 (% ± SD)
(1R,2S)-(-)-Ephedrine	124	75.87 ± 1.57	90.19 ± 0.39
(1S,2S)-(+)-Pseudoephedrine	4974	30.30 ± 1.68	52.21 ± 3.41
(1S,2R)-(+)-Norephedrine	132	74.53 ± 2.76	90.30 ± 0.53
(1R,2R)-(-)-Norpseudoephedrine	5020	46.71 ± 3.27	56.93 ± 5.30
(1R,2S)-(-)-N-Methylephedrine	27850	69.49 ± 1.62	86.61 ± 2.59
(1S,2S)-(+)-N-Methylpseudoephedrine	28890	73.84 ± 0.35	88.92 ± 0.68

Table 2

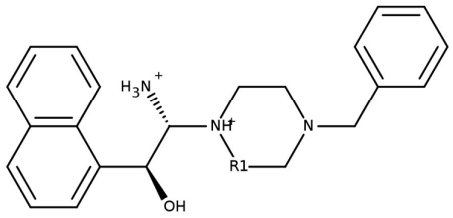

Norephedrine-naph-dev-199

Norephedrine derivative	R1 substituent	XP GScore (Kcal/mol)
199-279	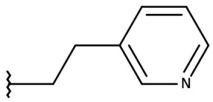	-12.520
199-701	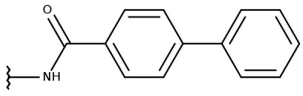	-12.345
199-303	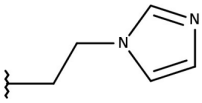	-11.770
199-93	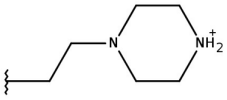	-11.373

Table 3

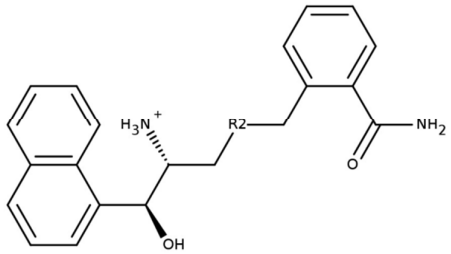

Norephedrine-naph-dev-443

Norephedrine derivative	R2 substituent	XP GScore (Kcal/mol)
443-182	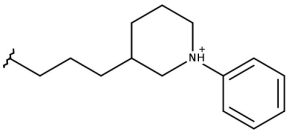	-11.763
443-177	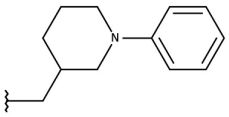	-11.754

Supporting information for

Ephedrine as a lead compound for the development of new DPP-IV inhibitors

Table S1. Bioactivity data in human targets for the six *Ephedra* alkaloids under study. No activity data was found for N-methylpseudoephedrine in the bibliography.

Target tested	Ephedrine	Pseudoephedrine	Norephedrine	Norpseudoephedrine	N-Methylephedrine
α1A-adrenoceptor	pK_i = 4.6 [1,2] pK_i = 5.0 [3]	pK_i = 4.2 [3]	pK_i = 5.1 [3]	pK_i = 4.6 [3]	pK_i = 4.2 [3]
α1B-adrenoceptor	pK_i = 4 [1,2] pK_i < 3 [3]	pK_i < 3 [3]			
α1D-adrenoceptor	pK_i = 4.3 [1] pK_i = 4.3 [3]	pK_i < 3 [3]			
α2A-adrenoceptor	pK_i = 6.1 [1,2] pK_i = 4.8 [3]	K_i = 2011 nM [4] pK_i = 4.2 [3]	pK_i = 6.6 [8] K_i = 3024 nM [4] pK_i = 5.2 [3]	pK_i = 4.3 [3]	pK_i = 4.2 [3]
α2B-adrenoceptor	pK_i = 5.6 [1,2] K_i = 648 nM [4] pK_i = 4.8 [3]	K_i = 1870 nM [4] pK_i = 4.4 [3]	K_i = 3940 nM [4]		pK_i = 4.3 [3]
α2C-adrenoceptor	pK_i = 5.1 [1,2] K_i = 708 nM [4] pK_i = 4.8 [3]	K_i = 1220 nM [4] pK_i = 4.2 [3]	K_i = 597 nM [4] pK_i = 5.0 [3]	pK_i = 4.5 [3]	pK_i = 4.1[3]
β2-adrenoceptor	K_d = 2830 nM [5] EC_{50} = 565 nM [5].				

Solute carrier family 22	IC_{50} = 29 μM [6]▪	IC_{50} = 4.2 mM [7]▪

Table S2. Commercialized gliptins sorted by year of authorization by health agencies.

Compound	Year of authorization by health agencies	Developed by	XP GScore (kcal/mol)[1]
Sitagliptin	FDA, 2006 EMA, 2007	Merck & co.	-8.096 (1X70)
Vildagliptin[2]	EMA, 2007	Novartis	
Saxagliptin[2]	FDA, 2009 EMA, 2009	AstraZeneca and Bristol-Myers Squibb	
Alogliptin	Japan, 2010 FDA, 2013	Takeda Pharmaceutical Company	-9.237 (3G0B)
Linagliptin	FDA, 2011	Boehringer Ingelheim	-10.833 (2RGU)
Teneligliptin	Japan, 2012 Korea, 2014	Mitsubishi Tanabe Pharma	-9.564 (3VJK)
Gemigliptin[3]	Korea, 2012	LG Life Sciences	
Anagliptin	Japan, 2012	Sanwa Kagaku Kenkyusho Co., Ltd. and Kowa Company, Ltd	-8.096 (3WQH)
Trelagliptin	Japan, 2015	Takeda Pharmaceutical Company	-10.018 (5KBY)
Evogliptin[3]	Korea, 2015	Dong-A Pharmaceutical	
Omariglitpin	Japan, 2015	Merck & co.	-7.611 (4PNZ)[4]

[1]XP GScore for the Glide refinement of the experimental pose of the corresponding gliptin at the PDB file indicated in parenthesis. This calculation was performed only for gliptins not covalently bound to DPP-IV.

[2]Gliptin covalently bound to Ser630.

[3]No crystallized protein-ligand complex available at the PDB.

[4]Crystallized protein-ligand complex with fluoroomarigliptin and not with omarigliptin.

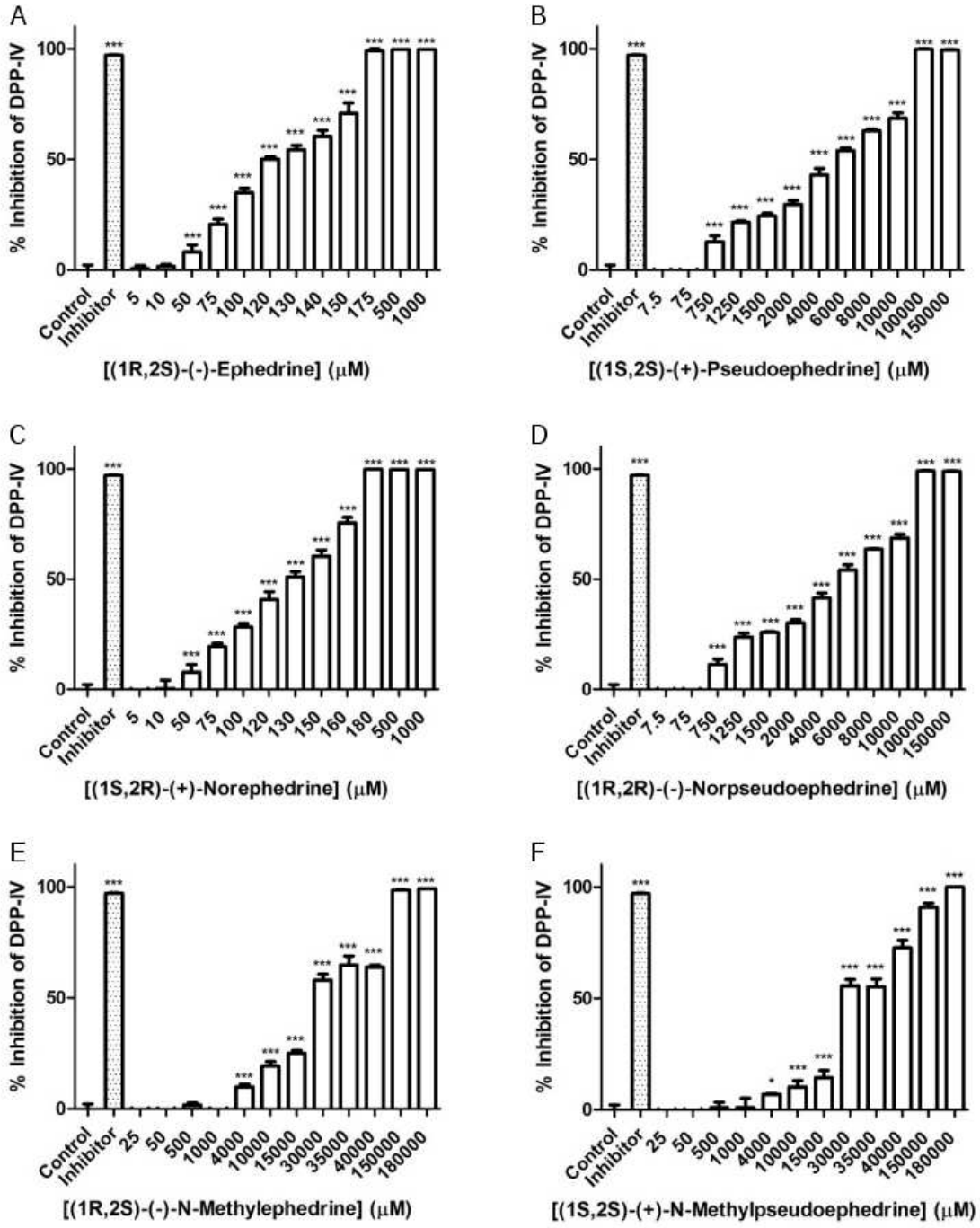

Figure S1

Dose-response of the six pure molecules tested at different concentrations to inhibit DPP-IV. *p<0.05 compared with the control. One-Way ANOVA followed by Bonferroni's Multiple Comparison Test. Data is expressed as mean ± SD of three replicates.

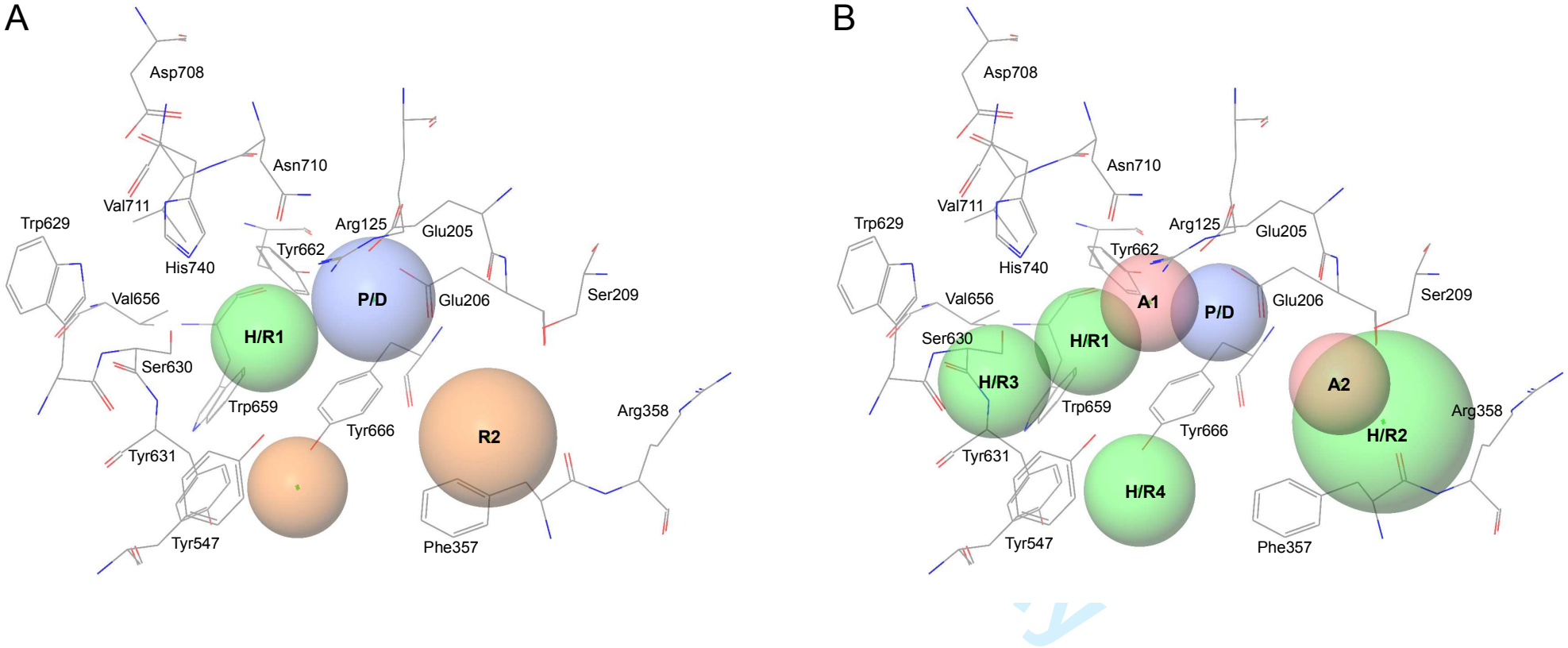

Figure S2. Comparison of the structure-based pharmacophore used in this paper (panel **A**) and the common structure-based pharmacophore used by us in previous studies (panel **B**). Main differences between them are: **(a)** optional sites **A1**, **A2** and **H/R3** are not considered now; **(b)** the optional **H/R2** and **H/R4** sites are now the **R2** and the **P/R3** sites, respectively; and **(c)** tolerances were readjusted using, as reference, more co-crystallized DPP-IV inhibitor complexes than in

the original pharmacophore.

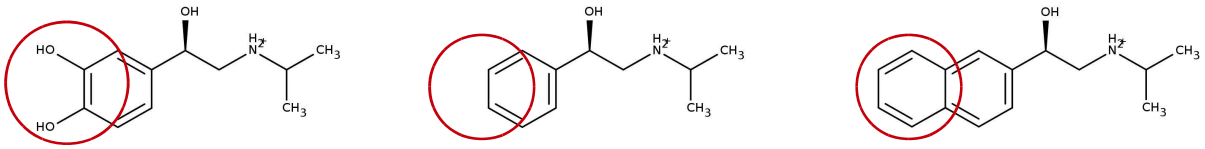

Isoprenaline
(agonist)
pX = 10.8

2-(isopropylamino)-1-phenylethanol
(agonist)
pX = 5.4

Pronethalol
(antagonist)

Figure S3. Chemical structure of selected ligands that interact with β_2 adrenergic receptor: isoprenaline (agonist) [9]▪ , 2-(isopropylamino)-1-phenylethanol (agonist) [10]▪ and pronethalol (antagonist).

1. Craig D, Forray C, Gluchowski C, Branchek T. US5610174 A1 - Use of α-1C-selective adrenoceptor agonists for the treatment of urinary incontinence. (1997).

2. Craig D, Forray C, Gluchowski C, Branchek T. WO1996/38143 - The use of α-1C-selective adrenoceptor agonists for the treatment of urinary incontinence. (1996).

3. Ma G, Bavadekar SA, Davis YM, *et al.* Pharmacological effects of ephedrine alkaloids on human α_1- and α_2-adrenergic receptor subtypes. *J. Pharmacol. Exp. Ther.* 322(1), 214–21 (2007).

4. Rothman RB, Vu N, Partilla JS, *et al. In vitro* characterization of ephedrine-related stereoisomers at biogenic amine transporters and the receptorome reveals selective actions as norepinephrine transporter substrates. *J. Pharmacol. Exp. Ther.* 307(1), 138–45 (2003).

5. January B, Seibold A, Whaley B, *et al.* β_2-adrenergic receptor desensitization, internalization, and phosphorylation in response to full and partial agonists. *J. Biol. Chem.* 272(38), 23871–9 (1997).

6. Suhre WM, Ekins S, Chang C, Swaan PW, Wright SH. Molecular determinants of substrate/inhibitor binding to the human and rabbit renal organic cation transporters hOCT2 and rbOCT2. *Mol. Pharmacol.* 67(4), 1067–77 (2005).

7. Rytting E, Audus KL. Novel organic cation transporter 2-mediated carnitine uptake in placental choriocarcinoma (BeWo) cells. *J. Pharmacol. Exp. Ther.* 312(1), 192–8 (2005).

8. Altenbach RJ, Khilevich A, Kolasa T, *et al.* Synthesis and structure−activity studies on N-[5-(1H-Imidazol-4-yl)-5,6,7,8-tetrahydro-1-naphthalenyl]methanesulfonamide, an imidazole-containing α_{1A} -adrenoceptor agonist. *J. Med. Chem.* 47(12), 3220–3235 (2004).

9. Kahsai AW, Xiao K, Rajagopal S, *et al.* Multiple ligand-specific conformations of the β_2-adrenergic receptor. *Nat. Chem. Biol.* 7(10), 692–700 (2011).

10. Grana E, Lilla L, Pratesi P, La Manna A, Villa L. Chemical structure and biological activity of catecholamines. 3. Exchange of the phenolic hydroxyls with other substitutents. *Farmaco. Sci.* 21(1), 4–15 (1966).